

On the cross-streamline lift of microswimmers in viscoelastic flows

Akash Choudhary^{1*} and Holger Stark^{1†}

¹*Institute of Theoretical Physics, Technische Universität Berlin, 10623 Berlin, Germany*

The current work studies the dynamics of a microswimmer in pressure-driven flow of a weakly viscoelastic fluid. Employing the second-order fluid model, we show that the self-propelling swimmer experiences a viscoelastic swimming lift in addition to the well-known passive lift that arises from its resistance to shear flow. Using the reciprocal theorem, we evaluate analytical expressions for the swimming lift experienced by neutral and pusher/puller-type swimmers and show that they depend on the hydrodynamic signature associated with the swimming mechanism. We find that for neutral swimmers focusing towards the centerline is accelerated by two orders of magnitude, while for force-dipole swimmers no net modification in cross-streamline migration occurs.

Biological microswimmers are ubiquitous in polymeric media such as cervical, bronchial, and intestinal mucus films [1, 2]. During the generation of biofilms, detrimental to bio-engineering and industrial processes, most bacteria release a mixture of proteins, DNA, and polysaccharides, endowing the fluid with viscoelastic properties [3, 4], which significantly alter the swimmer's dynamics [5]. Pathogens like ulcer-causing *Helicobacter pylori* thrive by altering the rheology of mucus lining in stomach [6]. Recent theoretical and experimental studies on the dynamics of motile microorganisms in Newtonian flows have revealed their rich dynamics and ability to swim against fluid flows, which aids in seeking nutrients and in reproduction [7–14].

Although recent works have provided insights in self-propulsion in non-Newtonian environments [14–31], few have studied the impact of fluid rheology on the dynamics of microswimmers in confined flows [32–34]. Mathijssen *et al.* [32] developed a model to predict the dynamical states of microswimmers in non-Newtonian Poiseuille flows. Employing a second-order fluid model, they demonstrated that normal-stress differences reorient the swimmers to cause centerline upstream migration (rheotaxis). This suggests that non-Newtonian properties can help microorganisms evade the boundary accumulation, prevalent in quiescent Newtonian fluids [35, 36].

The evidence of centerline reorientation of microswimmers can be traced back to pioneering works on viscoelastic focusing of passive particles in Poiseuille flows [37–39]. These studies showed that normal stresses exert a lift force that focuses the particles on the centerline. Ho and Leal [39] used the reciprocal theorem and derived an analytical expression for this lift in weakly elastic Boger fluids. The study suggested that the hydrodynamic disturbances around the particle produces a hoop stress that, in the presence of non-uniform shear rate, generates a cross-streamline lift. Recent progress in electrophoresis [40–42] has also shed light on the importance of hydrodynamic disturbances in determining these lift forces.

Active microswimmers, as opposed to passive parti-

cles, generate additional disturbance flow fields in the fluid due to their self-propulsion. Therefore, the associated lift force or velocity should also have an active component that is characteristic of the self-propulsion mechanism. Since this component is absent in the recently proposed models [32], in this communication we derive the ‘swimming lift’ in a second-order fluid (SOF), and show how it affects the dynamics of a microswimmer in the Poiseuille flow of a viscoelastic fluid. We choose the SOF model because it provides an asymptotic approximation for a majority of slow and slowly varying viscoelastic flows [43, 44].

Figure 1 shows a spherical swimmer of radius a at position \mathbf{r} that self-propels with velocity $\mathbf{v}_s = v_s \mathbf{p}$ in a two-dimensional pressure-driven flow $\mathbf{v}_f = v_m [1 - (x/w)^2] \mathbf{e}_z$, where v_m is the maximum flow velocity and w is the half channel width. The flow profile of the second-order fluid is identical to Poiseuille flow but the pressure field varies in x -direction [39]. In the absence of noise, the swimmer's dynamics is governed by

$$\dot{\mathbf{r}} = \mathbf{p} + \bar{\mathbf{v}}_f + \mathcal{F}(x, \mathbf{p}) \mathbf{e}_x, \quad \dot{\mathbf{p}} = \frac{1}{2} (\nabla \times \bar{\mathbf{v}}_f) \times \mathbf{p}, \quad (1)$$

where the velocities are non-dimensionalized by swimming speed v_s , lengths by w , and time by w/v_s . \mathcal{F} denotes the total viscoelastic lift velocity, which comprises the passive and swimming lift. Below, we derive the analytical expressions for the lift velocities. We note that normal stresses also modify the particle rotation and the drift velocity along the channel axis. We evaluated these modifications and found that they do not play a significant role in determining the swimmer dynamics.

The inertia-less or creeping flow hydrodynamics is governed by the continuity equations for mass and momentum, which we formulate here in the co-moving swimmer frame $\{\tilde{x}, \tilde{y}, \tilde{z}\}$ as:

$$\tilde{\nabla} \cdot \mathbf{V} = 0, \quad \tilde{\nabla} \cdot \mathbf{T} = 0 \quad (2)$$

in order to calculate the viscoelastic lift velocity. Length, velocity, and pressure in (2) are non-dimensionalized by a , κv_m , and $\mu \kappa v_m / a$, respectively. Here, κ is the particle to channel width ratio ($a/2w$) and μ is the fluid viscosity. In the above equation, \mathbf{T} is the total stress tensor of a second-order fluid and thus has the form [44]:

* a.choudhary@campus.tu-berlin.de

† holger.stark@tu-berlin.de

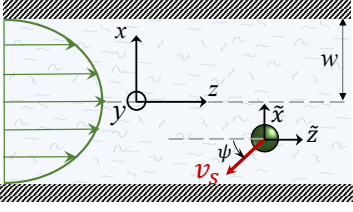


FIG. 1. A spherical microswimmer with velocity $v_s \mathbf{p}$ moves in a pressure-driven flow of a second-order fluid inside a channel with half width w . The coordinate frame $\{\tilde{x}, \tilde{y}, \tilde{z}\}$ co-moves with the swimmer.

$\mathbf{T} = -P\mathbf{I} + 2\mathbf{E} + \text{Wi}\mathbf{S}$. Here, \mathbf{E} denotes the rate of strain tensor and $\text{Wi} = (\Psi_1 + \Psi_2)G/\mu$ is the shear based Weissenberg number, where μ is the viscosity, $G = v_m/2w$ characterizes the shear rate in the background flow, and Ψ_1, Ψ_2 represent the dimensional steady-shear normal stress coefficients that are measured experimentally [44].

The polymeric stress tensor $\mathbf{S} = 4\mathbf{E} \cdot \mathbf{E} + 2\delta\mathbf{E}^\Delta$ is nonlinear in \mathbf{E} and contains the lower-convected time derivative of \mathbf{E} denoted by Δ . The viscometric parameter $\delta = -\Psi_1/2(\Psi_1 + \Psi_2)$ generally varies from -0.5 to -0.7 for most viscoelastic fluids [45–47].

We now focus on determining the lift velocity of a microswimmer that disturbs the background flow in two ways. First of all, the microswimmer resists straining by the flow and second, it generates a flow field characteristic of its swimming mechanism, for which we first take a source-dipole swimmer. We split the full velocity field ($\mathbf{V} = \mathbf{v}^\infty + \mathbf{v}$) into background flow field \mathbf{v}^∞ and disturbance field \mathbf{v} . Substituting this in the governing equations (2) yields:

$$\tilde{\nabla} \cdot \mathbf{v} = 0, \quad -\tilde{\nabla} p + \tilde{\nabla}^2 \mathbf{v} = -\text{Wi}(\tilde{\nabla} \cdot \mathbf{s}), \quad (3)$$

where \mathbf{s} is the polymeric stress tensor associated with the disturbance flow field (elaborated in the electronic supplementary material ESI). Assuming weak viscoelasticity, we perform a perturbation expansion in Wi and divide Eq. (3) into two problems: the Stokes equation for the zeroth order of the disturbance field and $-\tilde{\nabla} p_1 + \tilde{\nabla}^2 \mathbf{v}_1 = -\tilde{\nabla} \cdot \mathbf{s}_0$ at first order. Following earlier works on viscoelastic lift [39, 41], we use the reciprocal theorem to attain the lift velocity from the first-order problem

$$\mathcal{F} = -\frac{\text{Wi}}{6\pi} \int_{V_f} \mathbf{s}_0 : \tilde{\nabla} \mathbf{u}^t dV. \quad (4)$$

Here, \mathbf{u}^t is the auxiliary or test velocity field that belongs to a forced particle moving along the x -direction with unit velocity in a Newtonian fluid. The polymeric stress \mathbf{s}_0 corresponds to the Stokes solution \mathbf{v}_0 of the microswimmer consisting of (i) a source-dipole field, which we attain from the squirmer model [48–50], $\mathbf{v}_0^{\text{swim}} = \frac{v_s \mathbf{p}}{2\tilde{r}^3} \cdot \left[\frac{3\tilde{r}\tilde{r}}{\tilde{r}^2} - \mathbf{I} \right]$, and (ii) the passive disturbance field $\mathbf{v}_0^{\text{passive}}$, which is led by the stresslet; higher order

terms are obtained from Lamb’s general solution [51]. Using the corresponding \mathbf{s}_0 in Eq. (4), results in the viscoelastic lift velocity given in units of v_s :

$$\mathcal{F}(x, \psi) = \text{Wi} \left[\frac{80}{9} x \bar{v}_m \kappa^2 (1 + 3\delta) - x(1 + \delta) \cos \psi \right]. \quad (5)$$

The first component in Eq. (5) is the passive lift $\mathcal{F}_{\text{passive}}$ [39]. By fixing δ to a widely-used value of -0.5 (*i.e.* $\Psi_2 = 0$), we observe that $\mathcal{F}_{\text{passive}}$ focuses the particle towards the centerline. The second component is the swimming lift $\mathcal{F}_{\text{swim}}$ that arises due to the source-dipole disturbance created by the neutral swimmer. We note two striking features of $\mathcal{F}_{\text{swim}}$: the dependence on swimmer orientation through $\cos \psi$ and that its magnitude is larger by a factor κ^{-2} compared to the first term¹.

Now, we substitute \mathcal{F} into the dynamic equations (1) and examine the effect of $\mathcal{F}_{\text{swim}}$ on the microswimmer dynamics. We find two fixed points in the $x - \psi$ plane at $x = 0$, with the microswimmer oriented upstream ($\psi = 0$) or downstream ($\psi = \pm\pi$). A linear stability analysis provides the following eigenvalues for these fixed points:

$$\begin{aligned} \lambda_1 &\approx \frac{\text{Wi}}{18} [-9(1 + \delta) + 80(1 + 3\delta)\kappa^2 \bar{v}_m] \pm i \bar{v}_m^{1/2}, \\ \lambda_2 &\approx \frac{\text{Wi}}{18} [9(1 + \delta) + 80(1 + 3\delta)\kappa^2 \bar{v}_m] \pm \bar{v}_m^{1/2}. \end{aligned} \quad (6)$$

For a typical value of $\delta = -0.5$ and weak viscoelasticity limit ($\text{Wi} \ll 1$), the downstream swimming corresponds to a saddle fixed point (λ_2), while the upstream swimming along $x = 0$ corresponds to a stable fixed point (λ_1). For $\delta = -0.5$, the sign of the real part of λ_1 shows that both swimming and passive lift components stabilize the upstream swimming. However, the strong swimming lift can help the neutral microswimmer attain centerline

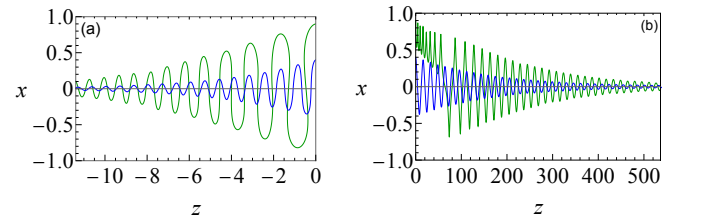


FIG. 2. Trajectories showing the centerline focusing of a neutral (source-dipole) swimmer oriented upstream while (a) swimming upstream ($\bar{v}_m = 0.9$) and (b) drifting downstream ($\bar{v}_m = 8$). Other parameters: $\text{Wi} = 0.1$, $\kappa = 0.1$, $\delta = -0.5$. The blue and green trajectories only differ in the initial condition x_0 .

¹The correction to the drift velocity in z -direction is $-\text{Wi} x \kappa \sin \psi (1 + \delta)$, and the correction to rotation is found to be $-\frac{8}{3} \text{Wi} \kappa \sin \psi$. We verified that these modifications do not alter the dynamics neither qualitatively nor quantitatively and thus neglect their contributions for simplicity. Details are provided in the ESI.

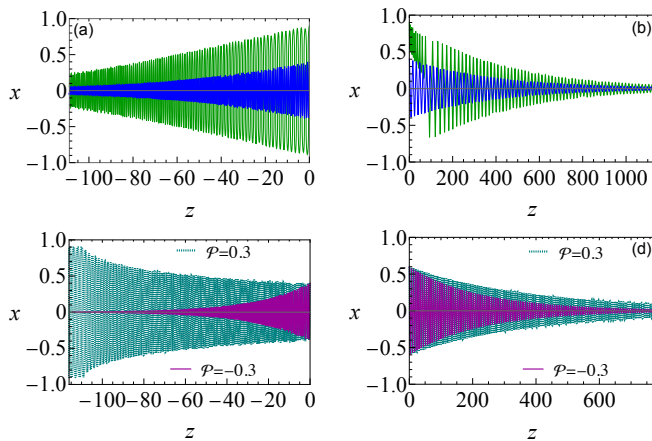


FIG. 3. Trajectories showing the centerline focusing of pusher/puller in (a) upstream swimming ($\bar{v}_m = 0.9$) and (b) downstream drifting ($\bar{v}_m = 8$). (c) Upstream ($\bar{v}_m = 0.9$) and (d) downstream trajectories ($\bar{v}_m = 3$) with hydrodynamic wall interactions (8) incorporated. We employ hard-core repulsion at the walls. Other parameters: $Wi = 0.1$, $\kappa = 0.1$, $\delta = -0.5$.

equilibrium more rapidly by a relaxation factor of κ^{-2} , as also shown in the trajectories of Fig.2 that are evaluated by substituting (5) in (1).

Now, we shift our attention from neutral squirmers to flagellated microorganisms, such as *E. coli* and *Chlamydomonas*, that generate a force-dipole field at the leading order [35, 52]: $\mathbf{v}_0 = \mathcal{P}\mathbf{r}\left[\frac{-1}{r^3} + 3\frac{(\mathbf{r}\cdot\mathbf{p})^2}{r^5}\right]$. Here \mathcal{P} is the force-dipole strength in units of $8\pi\mu a^2 v_s$, which depends on the swimming mechanism [35, 53, 54]. Earlier studies on *E. coli* [54, 55] and *Chlamydomonas* [56] suggest that $|\mathcal{P}|$ varies roughly between 0.04 - 0.3. Following the procedure outlined for a source-dipole swimmer, we obtain the swimming lift velocity of the force-dipole swimmer as

$$\mathcal{F}_{\text{swim}} = (8/3)Wi\kappa\mathcal{P}(1 + 3\delta)\sin 2\psi, \quad (7)$$

and find it to depend on the constant curvature in Poiseuille flow, as detailed in ESI. Although this lift is larger than $\mathcal{F}_{\text{passive}}$ by a factor κ^{-1} , there is no net lateral motion because the pure angular dependence cancels out on average as the particle tumbles continuously. The trajectories in Fig.3 (a) and (b) show the dynamics of a force-dipole swimmer; the focusing along the centerline is purely due to $\mathcal{F}_{\text{passive}}$.

So far we have neglected the hydrodynamic interactions of microswimmers with the bounding channel walls. For force-dipole swimmers, the hydrodynamic wall interactions add a modification of order κ^2 and κ^3 to the evolution equations of position and orientation, respectively

[10, 57]:

$$\dot{x} = -\sin\psi + \mathcal{F} - \frac{3\mathcal{P}(3\sin^2\psi - 1)}{8}\kappa^2\left[\frac{1}{(1-x)^2} - \frac{1}{(1+x)^2}\right],$$

$$\dot{\psi} = x\bar{v}_m - \frac{3\mathcal{P}\sin 2\psi}{16}\kappa^3\left[\frac{1}{(1-x)^3} + \frac{1}{(1+x)^3}\right]. \quad (8)$$

Upstream trajectories in Fig. 3(c) closely resemble the behavior reported previously for pure Newtonian fluids [10]. We observe that the hydrodynamic wall attraction of pushers [35] overcomes $\mathcal{F}_{\text{passive}}$ and results in swinging across the whole channel cross section, where the strong vorticity near the walls always re-orient the swimmer away from it. Pullers are repelled from walls [10] and, therefore, rapidly focus on the centerline. In contrast, for downstream drifting at large flow rates [Fig. 3(d)], $\mathcal{F}_{\text{passive}}$ dominates over the hydrodynamic wall interactions and all trajectories tend towards the centerline. We note that for source-dipole swimmers the hydrodynamic wall interactions are an order κ weaker, and therefore do not alter the trajectories qualitatively.

In conclusion, the current study analyzes microswimmers in weakly viscoelastic pressure-driven flows. For neutral and pusher/puller microswimmers, we derive an additional swimming lift velocity depending on the swimmer's hydrodynamic signature that adds to the passive viscoelastic lift [32, 39, 58, 59]. For source-dipole (neutral) swimmers, the swimming lift is two orders of magnitude stronger than the passive lift, which was considered alone in a recent study [32]. The current work shows that the swimming lift accelerates the centerline focusing. For force-dipole swimmers (pusher/puller), the swimming lift does not contribute to a net cross-streamline migration. Incorporating hydrodynamic wall interactions, we show that upstream swimming for weak flow strengths qualitatively follows the behavior in Newtonian fluids [10]: attraction of pushers towards the channel walls and repulsion of pullers. The downstream drifting along the centerline qualitatively remains the same as that of a passive particle.

These results suggest that normal stresses in viscoelastic fluids generated by the microswimmer's flow field can accelerate the centerline focusing. However, this strongly depends on the hydrodynamic signature of the microswimmer. Even for a weakly viscoelastic fluid ($Wi = 0.1$), we observe rapid focusing within a traveled distance of 10-500 times the channel width (Fig. 2), which amounts to ca. 1 - 50mm and is quite realistic for microfluidic channels. Thereby, this work contributes to the understanding of swimming in more realistic biological fluids. Furthermore, the current work offers several new directions to explore. For instance, elongated microswimmers perform Jeffery orbits in sheared Newtonian fluids [60]. In viscoelastic fluids the flow disturbances from swimming will alter the orientation evolution of these orbits and hence the swimmer dynamics [33]. Impact of shear-thinning fluids is also an interesting outlook, which can be achieved by the use of more detailed rheological models [44].

Support from Alexander von Humboldt fellowship is gratefully acknowledged.

- [1] S. S. Suarez and A. Pacey, *Hum. Reprod. Update* **12**, 23 (2006).
- [2] R. Levy, D. B. Hill, M. G. Forest, and J. B. Grotberg, *Integr. Comp. Biol.* **54**, 985 (2014).
- [3] A. Persat, C. D. Nadell, M. K. Kim, F. Ingremeau, A. Siryaporn, K. Drescher, N. S. Wingreen, B. L. Bassler, Z. Gitai, and H. A. Stone, *Cell* **161**, 988 (2015).
- [4] J. C. Conrad and R. Poling-Skutvik, *Annu. Rev. Chem. Biomol. Eng.* **9**, 175 (2018).
- [5] M. Jabbarzadeh, Y. Hyon, and H. C. Fu, *Phys. Rev. E* **90**, 043021 (2014).
- [6] J. P. Celli, B. S. Turner, N. H. Afdhal, S. Keates, I. Ghiran, C. P. Kelly, R. H. Ewoldt, G. H. McKinley, P. So, S. Erramilli, *et al.*, *Proc. Natl. Acad. Sci.* **106**, 14321 (2009).
- [7] F. Bretherton and N. M. V. Rothschild, *Proc. Biol. Sci.* **153**, 490 (1961).
- [8] J. Hill, O. Kalkanci, J. L. McMurry, and H. Koser, *Phys. Rev. Lett.* **98**, 068101 (2007).
- [9] R. Nash, R. Adhikari, J. Tailleur, and M. Cates, *Phys. Rev. Lett.* **104**, 258101 (2010).
- [10] A. Zöttl and H. Stark, *Phys. Rev. Lett.* **108**, 218104 (2012).
- [11] A. Zöttl and H. Stark, *Eur. Phys. J. E* **36**, 1 (2013).
- [12] C.-k. Tung, F. Ardon, A. Roy, D. L. Koch, S. S. Suarez, and M. Wu, *Phys. Rev. Lett.* **114**, 108102 (2015).
- [13] A. J. Mathijssen, N. Figueroa-Morales, G. Junot, É. Clément, A. Lindner, and A. Zöttl, *Nat. Comm.* **10**, 1 (2019).
- [14] E. Lauga, *The fluid dynamics of cell motility*, Vol. 62 (Cambridge University Press, 2020).
- [15] E. Lauga, *Phys. Fluids* **19**, 083104 (2007).
- [16] X. Shen and P. E. Arratia, *Phys. Rev. Lett.* **106**, 208101 (2011).
- [17] L. Zhu, E. Lauga, and L. Brandt, *Phys. Fluids* **24**, 051902 (2012).
- [18] O. S. Pak, L. Zhu, L. Brandt, and E. Lauga, *Phys. Fluids* **24**, 103102 (2012).
- [19] N. C. Keim, M. Garcia, and P. E. Arratia, *Phys. Fluids* **24**, 081703 (2012).
- [20] G. J. Elfring and E. Lauga, in *Complex fluids in biological systems* (Springer, 2015) pp. 283–317.
- [21] J. Sznitman and P. E. Arratia, in *Complex Fluids in Biological Systems* (Springer, 2015) pp. 245–281.
- [22] G. Li and A. M. Ardekani, *J. Fluid Mech.* **784**, R4 (2015).
- [23] C. Datt, L. Zhu, G. J. Elfring, and O. S. Pak, *J. Fluid Mech.* **784**, R1 (2015).
- [24] G. Li and A. M. Ardekani, *Phys. Rev. Lett.* **117**, 118001 (2016).
- [25] G. Li and A. M. Ardekani, *Eur. J. Comput. Mech.* **26**, 44 (2017).
- [26] T. R. Ives and A. Morozov, *Phys. Fluids* **29**, 121612 (2017).
- [27] C. Datt, G. Natale, S. G. Hatzikiriakos, and G. J. Elfring, *J. Fluid Mech.* **823**, 675 (2017).
- [28] Y. Zhang, G. Li, and A. M. Ardekani, *Phys. Rev. Fluids* **3**, 023101 (2018).
- [29] A. Zöttl and J. M. Yeomans, *Nat. Phys.* **15**, 554 (2019).
- [30] A. Choudhary, T. Renganathan, and S. Pushpavanam, *J. Fluid Mech.* **899**, A4 (2020).
- [31] J. P. Binagia, A. Phoa, K. D. Housiadas, and E. S. Shaqfeh, *J. Fluid Mech.* **900**, A4 (2020).
- [32] A. J. Mathijssen, T. N. Shendruk, J. M. Yeomans, and A. Doostmohammadi, *Phys. Rev. Lett.* **116**, 028104 (2016).
- [33] M. De Corato and G. D’Avino, *Soft Matter* **13**, 196 (2017).
- [34] A. M. Ardekani and E. Gore, *Phys. Rev. E* **85**, 056309 (2012).
- [35] A. P. Berke, L. Turner, H. C. Berg, and E. Lauga, *Phys. Rev. Lett.* **101**, 038102 (2008).
- [36] D. Smith, E. Gaffney, J. Blake, and J. Kirkman-Brown, *J. Fluid Mech.* **621**, 289 (2009).
- [37] A. Karnis and S. Mason, *J. Rheol.* **10**, 571 (1966).
- [38] F. Gauthier, H. Goldsmith, and S. Mason, *J. Rheol.* **15**, 297 (1971).
- [39] B. Ho and L. Leal, *J. Fluid Mech.* **76**, 783 (1976).
- [40] D. Li and X. Xuan, *Phys. Rev. Fluids* **3**, 074202 (2018).
- [41] A. Choudhary, D. Li, T. Renganathan, X. Xuan, and S. Pushpavanam, *J. Fluid Mech.* **898**, A20 (2020).
- [42] A. Choudhary, T. Renganathan, and S. Pushpavanam, *Phys. Rev. Fluids* **6**, 036701 (2021).
- [43] L. Leal, *J. Nonnewton. Fluid Mech.* **5**, 33 (1979), proceedings of the IUTAM Symposium on Non-Newtonian Fluid Mechanics.
- [44] R. B. Bird, C. F. Curtiss, R. C. Armstrong, and O. Hassager, *Dynamics of polymeric liquids, volume 1: fluid mechanics* (Wiley, 1987).
- [45] B. Caswell and W. Schwarz, *J. Fluid Mech.* **13**, 417 (1962).
- [46] L. Leal, *J. Fluid Mech.* **69**, 305 (1975).
- [47] D. L. Koch and G. Subramanian, *J. Nonnewton. Fluid Mech.* **138**, 87 (2006).
- [48] M. Lighthill, *Commun. Pure Appl. Math.* **5**, 109 (1952).
- [49] J. R. Blake, *J. Fluid Mech.* **46**, 199 (1971).
- [50] A. Zöttl and H. Stark, *Journal of Physics: Condensed Matter* **28**, 253001 (2016).
- [51] H. Lamb, Cambridge: Cambridge University Press, 1975, 6th ed. (1975).
- [52] T. Pedley and J. O. Kessler, *Annu. Rev. Fluid Mech.* **24**, 313 (1992).
- [53] K. Drescher, R. E. Goldstein, N. Michel, M. Polin, and I. Tuval, *Phys. Rev. Lett.* **105**, 168101 (2010).
- [54] K. Drescher, J. Dunkel, L. H. Cisneros, S. Ganguly, and R. E. Goldstein, *Proc. Nat.* **108**, 10940 (2011).
- [55] S. Chattopadhyay, R. Moldovan, C. Yeung, and X. Wu, *Proc. Natl. Acad. Sci.* **103**, 13712 (2006).
- [56] I. Minoura and R. Kamiya, *Cell Motil. Cytoskeleton* **31**, 130 (1995).
- [57] S. E. Spagnolie and E. Lauga, *J. Fluid Mech.* **700**, 105–147 (2012).
- [58] E. F. Lee, D. L. Koch, and Y. L. Joo, *J. Nonnewton. Fluid Mech.* **165**, 1309 (2010).
- [59] G. D’Avino, F. Greco, and P. L. Maffettone, *Annual Review of Fluid Mechanics* **49**, 341 (2017).
- [60] G. B. Jeffery, *Proc. Math. Phys. Eng.* **102**, 161 (1922).
- [61] S. Kim and S. J. Karrila, *Microhydrodynamics: principles and selected applications* (Courier Corporation, 2013).
- [62] T. Ishikawa, M. Simmonds, and T. J. Pedley, *J. Fluid Mech.* **568**, 119 (2006).
- [63] J. R. Blake, *J. Fluid Mech.* **46**, 199 (1971).
- [64] E. Guazzelli and J. F. Morris, *A physical introduction*

to suspension dynamics, Vol. 45 (Cambridge University Press, 2011).

[65] E. Lauga, *Langmuir* **20**, 8924 (2004).

Supplemental material for “On the cross-streamline lift of microswimmers in viscoelastic flows”

I. PROBLEM FORMULATION

The schematic in Fig. S1 (a) shows a neutrally buoyant spherical microswimmer suspended in pressure-driven flow of a polymeric fluid between two walls. In order to derive the expressions for the lift velocities, we work in a reference frame that translates with the swimmer ($\tilde{x}, \tilde{y}, \tilde{z}$). For simplicity, we temporarily drop the tilde notation. Fig. S1 (b) shows the non-dimensional description, where $s = d/2w$ and $s/\kappa = d/a$ is the distance from the bottom wall normalized by the particle radius a .

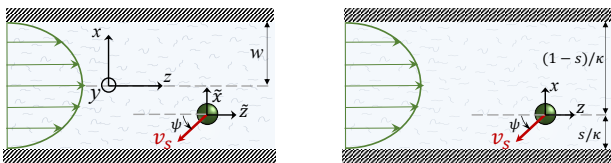


FIG. S1. (left) A spherical microswimmer self-propels with velocity $\mathbf{v}_s = v_s \mathbf{p}$ in a planar Poiseuille flow inside a channel with half width w . The coordinate frame $\{\tilde{x}, \tilde{y}, \tilde{z}\}$ co-moves with the swimmer. (right) Schematic with all lengths normalized by particle radius a . The tilde notation of the coordinates is shown to be dropped for brevity.

We split the actual velocity field into the background flow field \mathbf{v}^∞ and the disturbance field \mathbf{v} (*i.e.* $\mathbf{v}^{\text{actual}} = \mathbf{v} + \mathbf{v}^\infty$), and substitute in Eq. (2) of the article. The inertia-less hydrodynamics of the disturbance field is governed by the continuity and momentum equations in the co-moving swimmer frame $\{\tilde{x}, \tilde{y}, \tilde{z}\}$ as²:

$$\nabla \cdot \mathbf{v} = 0, \quad -\nabla p + \nabla^2 \mathbf{v} = -\text{Wi} (\nabla \cdot \mathbf{s}), \quad \text{where} \\ \mathbf{s} = 4(\mathbf{e} \cdot \mathbf{e} + \mathbf{w}) + 2\delta(\overset{\Delta}{\mathbf{e}} + \overset{\Delta}{\mathbf{w}}). \quad (\text{S1})$$

Here, \mathbf{e} is the rate of strain tensor for the disturbance flow $(\nabla \mathbf{v} + \nabla \mathbf{v}^\dagger)/2$, whereas \mathbf{w} , $\overset{\Delta}{\mathbf{e}}$ and $\overset{\Delta}{\mathbf{w}}$ are the different parts of the perturbation \mathbf{s} of the polymeric tensor due to the disturbance flow field \mathbf{v} :

$$\mathbf{w} = \mathbf{e}^\infty \cdot \mathbf{e} + \mathbf{e} \cdot \mathbf{e}^\infty, \\ \overset{\Delta}{\mathbf{e}} = \mathbf{v} \cdot \nabla \mathbf{e} + \mathbf{e} \cdot \nabla \mathbf{v}^\dagger + \nabla \mathbf{v} \cdot \mathbf{e}, \\ \overset{\Delta}{\mathbf{w}} = \mathbf{v}^\infty \cdot \nabla \mathbf{e} + \mathbf{e} \cdot \nabla \mathbf{v}^{\infty\dagger} + \nabla \mathbf{v}^\infty \cdot \mathbf{e} + \mathbf{v} \cdot \nabla \mathbf{e}^\infty \\ + \mathbf{e}^\infty \cdot \nabla \mathbf{v}^\dagger + \nabla \mathbf{v} \cdot \mathbf{e}^\infty, \quad (\text{S2})$$

where \mathbf{e}^∞ is the rate of strain tensor for the undisturbed flow, $\overset{\Delta}{\mathbf{e}}$ is the lower convected derivative of \mathbf{e} (also known

as the Rivlin-Eriksen tensor), \mathbf{w} is the ‘interaction tensor’ (arising from the interaction between background flow and disturbance field), and $\overset{\Delta}{\mathbf{w}}$ is its lower convected derivative.

The above equations are non-dimensionalized using $a, \kappa v_m, \mu \kappa v_m / a$ as the characteristic scales for length, velocity, and pressure, respectively. The definitions of these dimensional parameters a (particle size), $\kappa = a/2w$, and v_m (maximum flow velocity) are consistent with the communication article. In our case, \mathbf{v}^∞ is the undisturbed Poiseuille flow velocity in the frame of reference translating with the particle

$$\mathbf{v}^\infty = (\alpha + \beta x + \gamma x^2) \mathbf{e}_z - \mathbf{U}_p, \quad (\text{S3})$$

where \mathbf{U}_p is the total velocity of the swimmer, *i.e.*, swimming velocity \mathbf{v}_s plus advection due to the Poiseuille flow and the lift velocities. The constants α, β and γ are:

$$\alpha = 4s(1-s)/\kappa, \quad \beta = 4(1-2s), \quad \gamma = -4\kappa, \quad (\text{S4})$$

where β and γ represent the shear and curvature of the background flow, respectively. The boundary conditions of the disturbance flow field are

$$\mathbf{v} = \mathbf{v}_\theta + \boldsymbol{\Omega}_s \times \mathbf{r} - \mathbf{v}^\infty \quad \text{at } r = 1, \quad (\text{S5a})$$

$$\mathbf{v} = 0 \quad \text{at walls}, \quad (\text{S5b})$$

$$\mathbf{v} \rightarrow \mathbf{0} \quad \text{as } \{y, z\} \rightarrow \infty. \quad (\text{S5c})$$

Here, the walls are located at $x = -s/\kappa$ and $x = (1-s)/\kappa$, and \mathbf{v}_θ represents the prescribed tangential surface velocity of the spherical microswimmer.

II. PERTURBATION EXPANSION

We find the viscoelastic lift or migration velocities at $O(\text{Wi})$ using a regular perturbation expansion. For small values of Wi , the disturbance field variables are expanded as:

$$\xi = \xi_0 + \text{Wi} \xi_1 + \dots \quad (\text{S6})$$

Here, ξ is a generic field variable which represents velocity (\mathbf{v}), pressure (p), translational (\mathbf{U}_p) and angular velocity ($\boldsymbol{\Omega}_p$). We substitute (S6) in the equations governing the disturbance field (S1) and obtain the problem at $O(1)$ (*i.e.* Stokes problem) as

$$\left. \begin{aligned} \nabla \cdot \mathbf{v}_0 &= 0, \\ \nabla^2 \mathbf{v}_0 - \nabla p_0 &= \mathbf{0}, \\ \mathbf{v}_0 &= \mathbf{v}_\theta + \boldsymbol{\Omega}_{p0} \times \mathbf{r} - \mathbf{v}_0^\infty \quad \text{at } r = 1, \\ \mathbf{v}_0 &= 0 \quad \text{at walls}, \\ \mathbf{v}_0 &\rightarrow \mathbf{0} \quad \text{as } \{y, z\} \rightarrow \infty. \end{aligned} \right\} \quad (\text{S7})$$

²We follow a quasi-steady description because the time scales associated with cross-stream motions both due to swimming ($a/v_s \sim 1\text{s}$) and viscoelastic lift are much larger than the characteristic vorticity diffusion time ($a^2/\nu \sim 10^{-4}\text{s}$).

and at $O(\text{Wi})$ as:

$$\left. \begin{aligned} \nabla \cdot \mathbf{v}_1 &= 0, \\ \nabla^2 \mathbf{v}_1 - \nabla p_1 &= -\nabla \cdot \mathbf{s}_0, \\ \mathbf{v}_1 &= \mathbf{U}_{p1} + \boldsymbol{\Omega}_{p1} \times \mathbf{r} \quad \text{at } r = 1, \\ \mathbf{v}_1 &= \mathbf{0} \quad \text{at walls,} \\ \mathbf{v}_1 &\rightarrow \mathbf{0} \quad \text{as } \{y, z\} \rightarrow \infty. \end{aligned} \right\} \quad (\text{S8})$$

In (S7), $\mathbf{v}_0^\infty = (\alpha + \beta x + \gamma x^2) \mathbf{e}_z - \mathbf{U}_{p0}$.

Ho and Leal [39], in their seminal work, used the reciprocal theorem to derive a volume integral expression for the migration velocity associated with the $O(\text{Wi})$ equations (S8):

$$U_{\text{mig}} \equiv \text{Wi} \mathbf{U}_{p1} \cdot \mathbf{e}_x = -\frac{1}{6\pi} \text{Wi} \int_{V_f} \mathbf{s}_0 : \tilde{\nabla} \mathbf{v}^t dV. \quad (\text{S9})$$

The auxiliary or test field (\mathbf{v}^t, p^t) is associated with a sphere moving in the positive x -direction (towards the upper wall) with unit velocity in a quiescent fluid:

$$\mathbf{v}^t(\mathbf{r}) = \frac{3}{4} \left(\mathbf{e}_x + \frac{x\mathbf{r}}{r^2} \right) \frac{1}{r} + \frac{1}{4} \left(\mathbf{e}_x - \frac{3x\mathbf{r}}{r^2} \right) \frac{1}{r^3}. \quad (\text{S10})$$

The reciprocal theorem makes it relatively easy to find lift velocities at $O(\text{Wi})$, as we can solve the creeping flow problem (S7) using well-established methods [51, 61] and directly substitute its solution in (S9). In other words, we

do not need to solve the $O(\text{Wi})$ problem (S8) to obtain the $O(\text{Wi})$ lift.

III. VISCOELASTIC LIFT VELOCITY: SOURCE-DIPOLE SWIMMER

We now use expression (S9) for evaluating the swimming lift of a source-dipole swimmer. We explicitly choose the axisymmetric neutral squirmer, which has the surface velocity field $\mathbf{v}_\theta = B_1 \sin \theta \mathbf{e}_\theta$, where θ is the polar angle and \mathbf{e}_θ the corresponding base vector. The swimming velocity is directly related to this squirmer coefficient: $v_s = 2B_1/3$ [50, 62]. The solution to the $O(1)$ Stokes problem (S7) can be divided in swimming and passive disturbances. From the squirmer model [63], we obtain:

$$\begin{aligned} \mathbf{v}_0^{(1)\text{swim}} &= \frac{v_s \mathbf{p}}{2r^3} \cdot \left[\frac{3\mathbf{r}\mathbf{r}}{r^2} - \mathbf{1} \right] \\ &= \frac{v_s}{2r^3} \left[\cos \psi \left(\frac{3z\mathbf{r}}{r^2} - \mathbf{e}_z \right) + \sin \psi \left(\frac{3x\mathbf{r}}{r^2} - \mathbf{e}_x \right) \right]. \end{aligned} \quad (\text{S11})$$

Using Lamb's general solution [51], we obtain the passive disturbance

$$\begin{aligned} \mathbf{v}_0^{\text{passive}} &= B \left(-\mathbf{e}_z + \frac{3z\mathbf{r}}{r^2} \right) \frac{1}{r^3} + D \frac{zx\mathbf{r}}{r^5} + E \left(x\mathbf{e}_z + z\mathbf{e}_x - \frac{5xz\mathbf{r}}{r^2} \right) \frac{1}{r^5} \\ &+ F \left(\mathbf{e}_z - \frac{2x^2\mathbf{e}_z + z\mathbf{r}}{r^2} + \frac{2xz\mathbf{e}_x}{r^2} \right) \frac{1}{r^3} + G \left(\mathbf{e}_z - \frac{5x^2\mathbf{e}_z + 10xz\mathbf{e}_x + 13z\mathbf{r}}{r^2} + \frac{75zx^2\mathbf{r}}{r^4} \right) \frac{1}{r^3} \\ &+ H \left(\mathbf{e}_z - \frac{5x^2\mathbf{e}_z + 10xz\mathbf{e}_x + 5z\mathbf{r}}{r^2} + \frac{35zx^2\mathbf{r}}{r^4} \right) \frac{1}{r^5}, \end{aligned} \quad (\text{S12})$$

where the coefficients are defined as:

$$B = \frac{\gamma}{15}, \quad D = -\frac{5\beta}{2}, \quad E = -\frac{\beta}{2}, \quad F = \frac{\gamma}{3}, \quad G = -\frac{7\gamma}{120}, \quad H = \frac{\gamma}{8}. \quad (\text{S13})$$

The terms multiplying the coefficients B , D , E represent source-dipole, stresslet, and octupole singularities, respectively [61, 64]. The other disturbances (terms multiplying F , G , H) are further singularities in the multipole expansion, which arise due to the curvature γ in the background flow field together with the source dipole.

The tensor \mathbf{e}^∞ is yet unknown for the Poiseuille flow of Eq. (S3) in zeroth order of Wi . To calculate it, we note that the total velocity of the force-free swimmer in the Stokes regime is $\mathbf{U}_{p0} = \mathbf{v}_s + (\alpha + \gamma/3)\mathbf{e}_z$ (the second part is obtained by using Faxen's laws [61]). To complete the expression of \mathbf{v}_0^∞ , we substitute \mathbf{U}_{p0} in (S3), and obtain:

$$\mathbf{v}_0^\infty = (\beta x + \gamma x^2 - \gamma/3)\mathbf{e}_z - \mathbf{v}_s \quad (\text{S14})$$

which gives $[\mathbf{e}^\infty]_{xz} = [\mathbf{e}^\infty]_{zx} = (\beta + 2x\gamma)/2$.

Now, we evaluate the volume integral in Eq. (S9). Since the source-dipole field of the neutral swimmer decays quickly away from the swimmer ($\sim 1/r^3$), we can neglect the wall corrections in the volume integral of Eq. (S9). In the context of an electrophoretic source-dipole disturbance, Choudhary *et al.* [41] showed that the error generated from this neglect is dispensable. Integrating over the infinite space, we obtain the swimming lift velocity in units of v_s as

$$U_{\text{mig}} = \text{Wi} \left[(5/9)\beta\gamma(1 + 3\delta)\bar{v}_m\kappa + (1/4)\beta(1 + \delta)\cos\psi \right], \quad (\text{S15})$$

expressed in the co-moving frame of the swimmer. The first component is the passive lift velocity (identical to that obtained by Ho and Leal [39]), and the second component is the swimming-lift velocity that arises due to the source-dipole disturbance created by the neutral swimmer.

IV. VISCOELASTIC LIFT VELOCITY: FORCE-DIPOLE SWIMMER

As before, \mathbf{v}_0 is the combination of flow fields due to swimming and the passive disturbance. The latter is identical to (S12); for the swimmer, we take the force-dipole field from the studies on flagellated microswimmers [57, 65], where \mathcal{P} is the dipole strength normalized with $8\pi\mu a^2 v_s$:

$$\begin{aligned} \mathbf{v}_0^{(1)swim} &= \mathcal{P} \mathbf{r} \left[\frac{-1}{r^3} + 3 \frac{(\mathbf{r} \cdot \mathbf{p})^2}{r^5} \right] \\ &= \mathcal{P} \cos^2 \psi \left(\frac{-\mathbf{r}}{r^3} + \frac{3z^2 \mathbf{r}}{r^5} \right) + \mathcal{P} \sin^2 \psi \left(\frac{-\mathbf{r}}{r^3} + \frac{3x^2 \mathbf{r}}{r^5} \right) + \mathcal{P} \sin 2\psi \left(\frac{3xz \mathbf{r}}{r^5} \right). \end{aligned} \quad (\text{S16})$$

Substituting the above equation together with Eq. (S12) into Eq. (S9) and integrating over the infinite domain, we obtain (in the units of v_s):

$$U_{\text{mig}} = \text{Wi} [(5/9)\beta\gamma(1+3\delta)\bar{v}_m\kappa - (2/3)\mathcal{P}\gamma(1+3\delta)\sin 2\psi]. \quad (\text{S17})$$

The second component is the additional swimming-lift velocity that will be experienced by the force-dipole swimmer. Note that it depends on the curvature γ of the Poiseuille flow.

V. INERTIAL LIFT VELOCITIES IN THE CHANNEL FRAME

Here we provide the final expressions of the swimming and passive lift velocities in the channel frame of reference, which is used in the communication article. The conversion requires a transformation of particle-wall distance s/κ to the channel x coordinate (see Fig. 1); for x in units of w we then have $s = (1+x)/2$.

1. Swimming lift: Neutral microswimmer

Using the definition of β (S4) and $s = (1+x)/2$ in (S15), yields:

$$U_{\text{mig}} = \mathcal{F}_{\text{swim}} = -\text{Wi}(1+\delta)x \cos \psi. \quad (\text{S18})$$

2. Swimming lift: Pusher/puller microswimmer

Using the definition of γ (S4) in (S17), yields:

$$U_{\text{mig}} = \mathcal{F}_{\text{swim}} = \text{Wi}(8/3)(1+3\delta)\mathcal{P}\kappa \sin 2\psi \quad (\text{S19})$$

3. Passive lift:

Using the definition of β, γ (S4) and $s = (1+x)/2$ in the passive lift component, yields:

$$U_{\text{mig}} = \mathcal{F}_{\text{passive}} = \text{Wi}(80/9)(1+3\delta)x \bar{v}_m \kappa^2. \quad (\text{S20})$$

VI. PARTICLE DRIFT AND ROTATION MODIFICATION

To calculate the viscoelastic modification to drift and rotational velocity of the swimmer, we use the following two test fields (respectively):

$$\mathbf{v}^t(\mathbf{r}) = \frac{3}{4} \left(\mathbf{e}_z + \frac{z\mathbf{r}}{r^2} \right) \frac{1}{r} + \frac{1}{4} \left(\mathbf{e}_z - \frac{3z\mathbf{r}}{r^2} \right) \frac{1}{r^3}. \quad (\text{S21})$$

$$\mathbf{v}^t(\mathbf{r}) = \frac{x\mathbf{e}_z - z\mathbf{e}_x}{r^3}. \quad (\text{S22})$$

A. Source-dipole swimmer

Substituting (S21) in the volume integral (S9), we obtain the drift modification as:

$$U_{\text{drift}} = \frac{1}{4} \text{Wi} \beta v_s (1+\delta) \sin \psi. \quad (\text{S23})$$

Substituting (S22) in the volume integral (S9), we obtain the rotation modification as:

$$\mathbf{\Omega}_1 = \frac{2}{3} \text{Wi} \gamma v_s \sin \psi \mathbf{e}_y \quad (\text{S24})$$

B. Force-dipole swimmer

Similarly, for force-dipole swimmer, we obtain

$$U_{\text{drift}} = \frac{1}{12} \text{Wi} \gamma v_s (1+\delta) (-3+5 \cos \psi),$$

$$\mathbf{\Omega}_1 = \frac{2}{3} \text{Wi} \beta v_s (1+3\delta) \cos 2\psi.$$

Since these effects are an order of magnitude (in Wi) smaller than the flow speed and flow vorticity (respectively), they do not alter the swimmer dynamics.